excitation with photons of energies corresponding to the band-to-band transitions differ from those obtained after irradiation in the exciton bands.

ACKNOWLEDGMENT

We wish to thank Dr. R. Chen for helpful discussions.

[1]See, e.g., J. H. Parker, Phys. Rev. 124, 703 (1961); F. T. Goldstein, Phys. Status Solidi 20, 379 (1967); D. Pooley, and W. A. Runciman, Solid State Commun. 4, 351 (1966); J. D. Konitzer and H. N. Hersh, J. Phys. Chem. Solids 27, 771 (1966).

[2]D. Pooley, Proc. Phys. Soc. (London) 87, 245 (1966); 87, 257 (1966); H. N. Hersh, Phys. Rev. 148, 928 (1966).

[3]Y. Farge, J. Phys. Chem. Solids 30, 1375 (1969).

[4]M. Israeli and N. Kristianpoller, Solid State Commun. 7, 1131 (1969).

[5]J. E. Eby, K. J. Teegarden, and D. B. Dutton, Phys. Rev. 116, 1099 (1959).

[6]A similar effect of excitation of carriers with light in a region of high absorbance – however, into already existing traps – is presently being studied in our group. [R. Chen and present authors (unpublished).]

[7]W. Martienssen, J. Phys. Chem. Solids 2, 257 (1957).

[8]H. Pick, *Zahlenwerte und Funktionen* (Landolt-Börenstein, Berlin, 1955), Vol. I/4, p. 869.

[9]N. Itoh, B. S. H. Royce, and R. Smoluchowski, Phys. Rev. 138, 1766 (1965); R. Balzer, H. Peisel, and W. Waidelich, Phys. Status Solidi 31, K29 (1969).

PHYSICAL REVIEW B VOLUME 2, NUMBER 6 15 SEPTEMBER 1970

# Optical Properties of NiO and CoO†*

R. J. Powell‡ and W. E. Spicer
*Stanford Electronics Laboratories, Stanford University, Stanford, California* 94305
(Received 6 November 1969)

The optical reflectance spectra of the transition-metal oxides NiO and CoO have been measured over the energy range from 1 to 26 eV. The optical constants have been derived by means of a Kramers-Krönig analysis of their reflectance spectra. Structure in reflectance is found at 4.0, 4.8, 5.9, 7.2, 8.25, 12.8, 13.6, and 17.8 eV in NiO, and at 5.5, 7.5, 12.6, and 17.5 eV in CoO. The positions of high-energy structure in their absorption coefficients is consistent with maxima in their respective optical densities of states determined from photoemission data. Two alternative interpretations are given for the structure in NiO between 4.0 and 9.0 eV. One interpretation involves oxygen *p* and nickel *d* states in localized excitations, and the other involves the nickel *d* states and the "4*s*" band. Distinction between models on the basis of presently available photoconductivity data is found to be questionable.

## I. INTRODUCTION

The electronic structure of the low-mobility transition-metal compounds has become the subject of increased interest in recent years because of the rather diverse electrical and magnetic properties of these compounds and the recognition that they represent a considerable gap in our knowledge of the solid state.

The purpose of this work was to investigate a part of this field of study which has been the subject of considerable disagreement for some time; the electronic structure of the 3*d* transition-metal oxides. Notwithstanding the practical importance of these materials, their importance from a purely scientific view point lies in the difficulty of conceiving suitable models to explain their properties.

Studies of the optical constants in the ultraviolet and vacuum ultraviolet have proven to be a powerful method for determining details of the electronic structure of semiconductors and metals,[1–7] especially for materials for which meaningful band-structure calculations have been performed. In addition, the prior availability of the optical properties is often of considerable assistance to the theorist in making such calculations. A considerable amount of useful information can be extracted from the optical properties even though theoretical calculations are not available to assist in the interpretation. This is especially true when optical data are analyzed in conjunction with other experimental data such as photoelectron energy distributions.[8–11]

In this paper we present the results of reflec-

tance measurements on NiO and CoO over the photon energy range from 1.0 to 26.8 eV. The optical constants have been derived through the use of a Kramers-Kronig analysis of the reflectance data.

## II. EXPERIMENTAL DETAILS

### A. Samples and Preparation

Single crystals of NiO and CoO used in this work were cut from flame-fusion-grown boules. The reflectance samples were prepared by cleaving a 2-mm-thick wafer from a larger single crystal. Cleaving was accomplished by placing a tungsten carbide blade in contact with the crystal (properly oriented) and striking the blade lightly with a hammer. The samples were cleaved in air and fastened to a sample holder with a low-vapor-pressure Epoxy resin cement. Reflectance measurements were made on cleaved faces, except in one case; a polished sample of NiO was also measured.

### B. Experimental Apparatus

The source of monochromatic radiation for all measurements was a McPherson model 225, 1-m normal-incidence vacuum ultraviolet monochromator. Light was generated in a Hinterregger-type gas discharge lamp. Hydrogen was used in the discharge lamp for measurements in the photon energy range from 1 to 14 eV, and for the 14- to 26.8-eV range emission lines from argon, helium, and neon were used.

In order to obtain a quantitative determination of the optical constants of a material from reflectance measurements, it is necessary to measure its absolute reflectance. To accomplish this, the sample surface must be highly specular or a fraction of the incident light will be scattered and not intercepted by the detector during measurement of the reflected intensity. In addition, the sensitive surface of the detector should be uniform so that for a given intensity its response does not vary appreciably with the position, size, or orientation of the beam.

The reflectance measurement apparatus described below was designed so that with suitable precautions absolute reflectance may be measured.

Shown in Fig. 1 is a cutaway view of the measurement chamber which was used to obtain the reflectance spectra of NiO and CoO. This chamber was designed by Eden[12] of this laboratory to measure absolute reflectance as nearly as practical.

The sample and a phosphor-coated light pipe are mounted on a rotatable holder in such a manner that the distance to the sensitive surface of the light pipe (optical path length) remains the same in both incident and reflected measurement positions. The manner in which this is accomplished

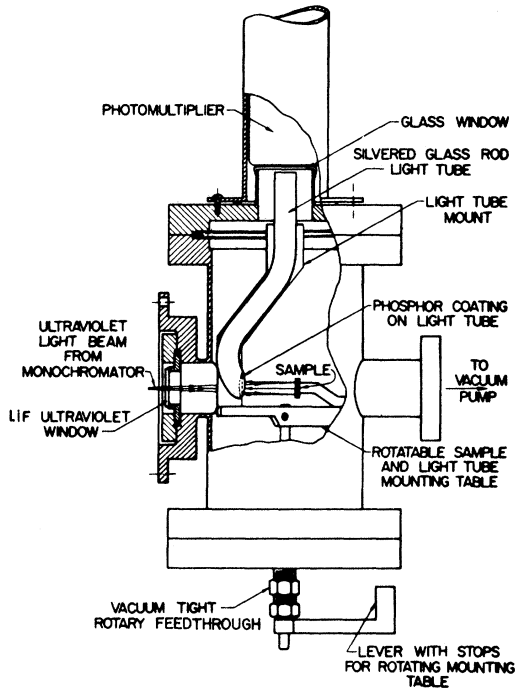


FIG. 1. Reflectivity measurement chamber of Eden (Ref. 12).

is easily understood upon reference to Fig. 2. Light falling upon the phosphor-coated surface of the light pipe is converted to the fluorescent wavelength of the phosphor, travels down the reflecting glass pipe, and is measured by a photomultiplier after passing through a glass window on the top flange of the vacuum chamber.

### C. Measurements

Throughout the photon energy range from 1 to 11 eV, suitable filters were used to ensure that higher-order responses of the diffraction grating were eliminated from the output. In addition, in the high-energy range (above 10 eV), filters of $CaF_2$ (for 10- to 12-eV range) and LiF (above 12 eV) were used to determine the presence and amount of lower-energy scattered light coming from the diffraction grating. This can sometimes be a serious problem since at high energies the source intensity becomes small and generally so does the sample reflectance. Thus, the normally small amount of lower-energy scattered light coupled with a usually higher sample reflectance at lower energies can give significant errors. Scattered light contributions were found to be insignificant except near 14 eV, where the hydrogen spectrum intensity is very small. At this photon energy, about 5% of the incident intensity passed

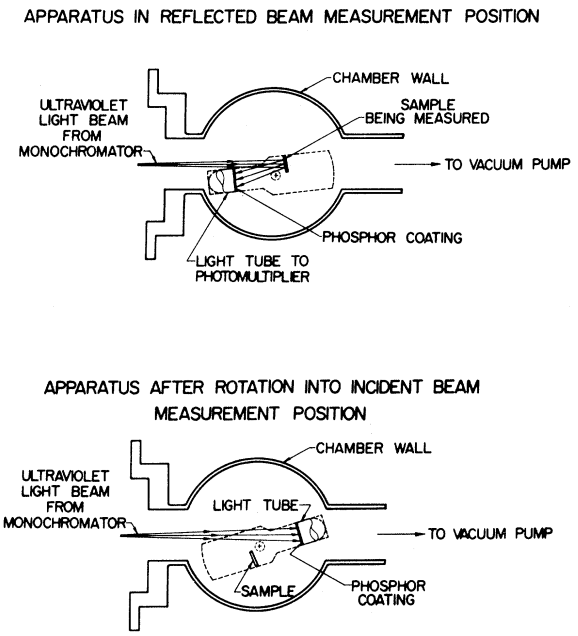


FIG. 2. Illustration of operation of reflectance chamber.

through a LiF filter (opaque beyond 12 eV). In this case it was found that the scattered contribution vanished when a $CaF_2$ filter (cutoff at 10 eV) was inserted, indicating that nearly all of the scattered light had photon energies above 10 eV. Hence, the scattered contribution is primarily from the Lyman-$\alpha$ line at 10.2 eV, since it is by far the most intense portion of the $H_2$ spectrum above 10 eV. Approximate correction for the scattered light can be made by subtracting from incident intensity the intensity remaining with the LiF filter in place and then subtracting from reflected intensity this scattered fraction multiplied by the sample reflectance at $\hbar\omega = 10.2$ eV. The scattered light intensity was checked during every reflectance measurement, since it depends primarily on the condition of the diffraction grating (amount of diffusion pump oil deposited, etc.) and can vary significantly with time.

Monochromator slits were kept small to provide a resolution of about 8 Å, and at each photon energy incident and reflected intensity measurements were made seconds apart followed by an incident check to minimize the effects of source intensity variations. Readings were made with an integrating digital voltmeter to improve accuracy and reduce the effects of noise, and several samples of both NiO and CoO were measured to ascertain the reproducibility of the results.

## III. NiO EXPERIMENTAL RESULTS

### A. NiO Reflectance Spectrum

The absolute reflectance of NiO was measured from one polished and two cleaved samples for photon energies ranging from 1.0 to 26.8 eV. Absolute reflectance was also measured at one wavelength using the beam of a helium-neon laser (1.96 eV) and a silicon solar-cell detector in order to provide a check on the chamber measurements and give an accurate value for the optical dielectric constant.

The spectrum of reflectance from a cleaved NiO crystal is shown in Fig. 3. The only part of this spectrum which has been previously reported[13] is the prominent peak at a photon energy of 4.0 eV (marked P4.0 in Fig. 3), where the reflectance reaches 32%. Proceeding to higher energies in Fig. 3, the next structure noted is a shoulder at 4.8 eV (S4.8). This shoulder was more prominent in another cleaved sample than it is in the one depicted in the figure. The next three pieces of structure in the reflectance, which occur at $\hbar\omega = 5.9$, 8.25 eV were clearly resolved in both cleaved samples, but not in the polished sample. Although P5.9 appears as a shoulder in Fig. 3, it was resolved as a definite peak in another sample.

The doublet peak (D12.8-D13.6) at $\hbar\omega = 12.8$, 13.6 eV and the final peak at $\hbar\omega = 17.8$ eV (P17.8) were identical in both cleaved and polished samples. The data-point increments were 0.1 eV for $1.0 \leq \hbar\omega \leq 12.6$ eV, 0.2 eV for $12.6 \leq \hbar\omega \leq 14.4$ eV, and for $\hbar\omega > 14.4$ eV data points were obtained at 16.8, 17.1, 18.45, 21.2, 21.4, and 26.8 eV. Consequently, the details are accurately known for $\hbar\omega \leq 14.4$ eV, but the detailed nature (i.e., possible splitting, etc.) of the peak P17.8 is not certain,

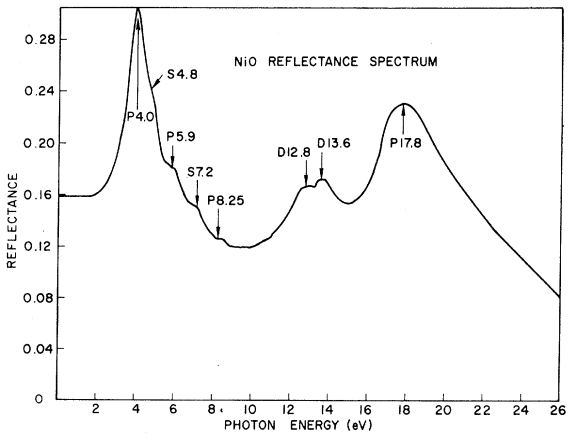


FIG. 3. Reflectance spectrum of NiO.

and other small structures may exist on the slopes of this peak.

A Kramers-Krönig analysis was performed on the reflectance data assuming constant reflectance from $\hbar\omega = 1.0$ to $\hbar\omega = 0$ eV[14] and extrapolating the high-energy reflectance to $\hbar\omega = 100$ eV.

The optical properties determined from the Kramers-Krönig analysis were found quite insensitive to the functional form of the high-energy extrapolation. The calculation was done using the method of infinite unit slopes of attenuation discussed by Thomas[15] (see Appendix). Using this method the functional dependence of reflectance between the last measured point ($\hbar\omega = 26.8$ eV) and $\hbar\omega = 100$ eV is $R = R\,(26.8)/(\hbar\omega - 26.8)^K$. The constant $K$ was adjusted to eliminate negative absorption coefficients for $\hbar\omega < 4.0$ eV (this is the usual practice – see Ref. 1).

As mentioned, the details of the reflectance peak at $\hbar\omega = 17.8$ eV are not known because of the coarseness of the data points in this region. To determine the dependence of lower-energy structure on the reflectance in this region, the data above $\hbar\omega = 14.4$ eV were eliminated and the reflectance was extrapolated (as previously described) from $\hbar\omega = 14.4$ eV to a small value at $\hbar\omega = 100$ eV, thus completely discarding the $\hbar\omega = 17.8$ eV peak. The effect on the optical constants of this rather gross change was to change somewhat their magnitudes at high photon energies (nearest the change). The shape and positions of structure were unaffected.

### B. Optical Constants of NiO

Two commonly used optical constants are presented in Figs. 4 and 5 for NiO. Figure 4 gives the real ($n$) and imaginary ($k$) parts of the complex refractive index ($N = n - ik$), and Fig. 5 depicts the

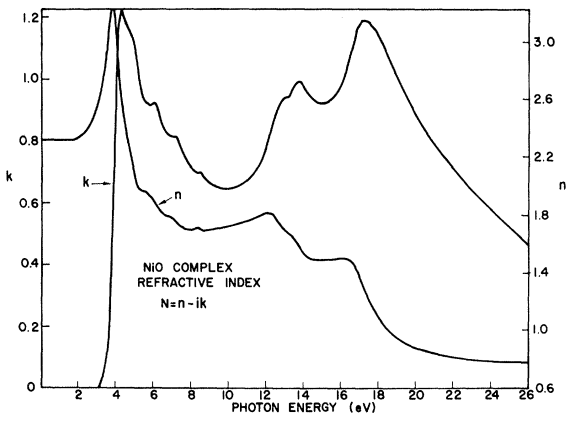


FIG. 4. Real and imaginary parts of the NiO complex refractive index (determined from the reflectance spectrum).

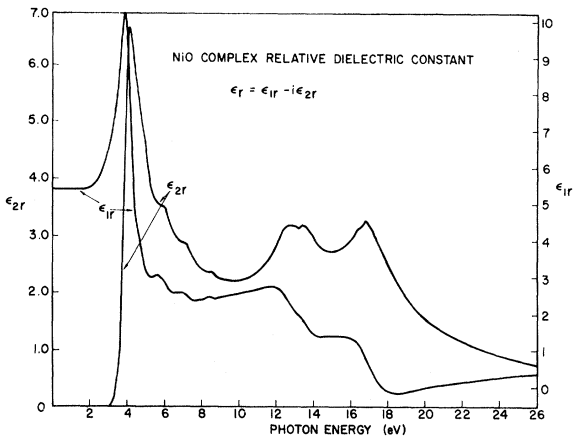


FIG. 5. Real and imaginary parts of the NiO complex. Relative dielectric constant (determined from the reflectance spectrum).

real ($\epsilon_{1r}$) and imaginary ($\epsilon_{2r}$) parts of the complex relative dielectric constant ($\epsilon_r = \epsilon_{1r} - i\epsilon_{2r}$). The structural features of the imaginary components of these constants are similar to the shape of the reflectance spectrum, but the actual positions of the peaks and shoulders are shifted in energy.

The real parts of $N$ and $\epsilon_r$ approach constant values at low photon energies. As shown in Table I, the values differ somewhat from some of those obtained by other workers. Table I summarizes the values for the refractive index and optical dielectric constant previously reported, along with the values determined from the present work. The

TABLE I. Refractive index and optical dielectric constant of NiO.

| Refractive Index $n$ | Optical dielectric constant $\epsilon_{1r} = n^2$ | Method | Ref. |
|---|---|---|---|
| 2.45 | 5.76 | Infrared reflectance (1 $\mu$) (experimental) | 16 |
| 2.38 | 5.7 | Calculated from damped oscillator model applied to lattice vibrational spectra | 17 |
| 2.26 | 5.12 (4.75) | Calculated from damped oscillator model applied to lattice vibrational spectra (4.75 is experimental) | 18 |
| 2.32 | 5.4 | Reflectance (experimental) | 13 |
| 2.33 | 5.43 | Reflectance ($\hbar\omega = 2.0$ eV) | Present work |

values obtained in this work are believed to be accurate to within ± 3% (at $\hbar\omega = 2.0$ eV), since they were obtained consistently for polished and cleaved crystals of different origins. Our values are within experimental uncertainty of the values obtained by Newman and Chrenko, [13] although they differ considerably from the experimental work of Rao and Smakula. [16] The rather wide range of values presented by them and their co-workers[16–18] should be noted.

A plot of the NiO optical-absorption coefficient is presented in Fig. 6. The photon energies at which structure shows are marked by the arrows in the figure. Note that the positions of the structure in the absorption coefficient are somewhat different than those of the reflectance spectrum of Fig. 3. This is an expected result, since reflectance depends on both the real and imaginary parts of the complex refractive index ($N = n - ik$) while the absorption coefficient depends on $k$ alone ($\alpha = 4\pi k/\lambda$).

Near the absorption edge, we can compare the present work with that of Doyle and Lonergan, [19] and Rossi and Paul[20] taken on NiO thin films. Optical density is related to absorption coefficient $\alpha$, reflectance $R$, and sample thickness $t$ by the following equation:

$$\text{optical density} = \log_{10}\left[\frac{e^{\alpha t}}{(1-R)^2}\right].$$

The optical density of NiO from 3.0 to 6.0 eV has been calculated from the absorption coefficient of Fig. 6 using a thickness of 2300 Å. A comparison of this optical density with that of the aforementioned absorption measurements is shown in Fig. 7. The data of Doyle and Lonergan and Rossi and Paul have been scaled to give the same optical density as our data at $\hbar\omega = 5.4$ eV, since these authors

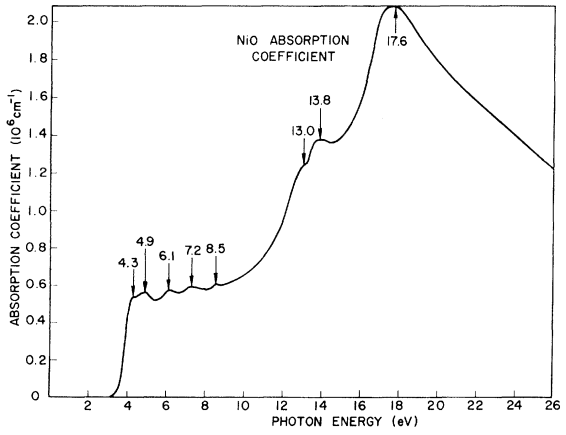


FIG. 6. Optical-absorption coefficient of NiO (determined from the reflectance spectrum).

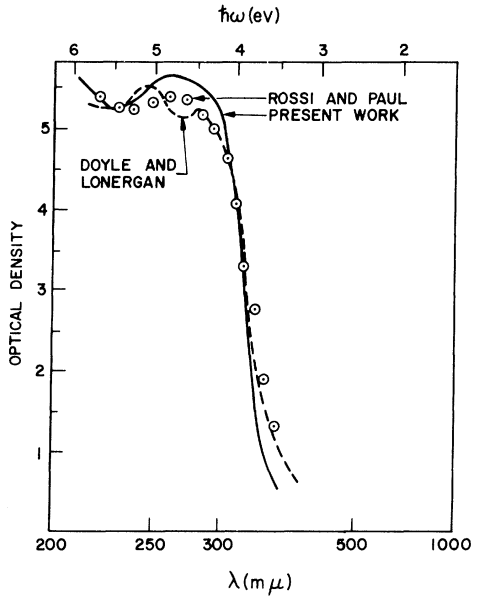


FIG. 7. Optical density of NiO for $\hbar\omega < 6$ eV. Dashed curve from data of Doyle and Lonergan (Ref. 19). Encircled points are data of Rossi and Paul (Ref. 20).

do not indicate their film thickness. The agreement is quite good in view of the relative insensitivity of reflectance to small changes in absorption.

Another useful quantity which may be obtained from the optical constants is $n_{eff}(\hbar\omega_0)$ which is the effective number of electrons per NiO molecule contributing to the optical absorption at photon energy $\hbar\omega_0$. This quantity is obtained from the sum rule[21]:

$$n_{eff}(\hbar\omega_0) = (2m/Ne^2\hbar^2)\int_0^{\hbar\omega_0} E\epsilon_{2r}(E)\,dE,$$

where $m$ is the free-electron mass and $N$ is the number of NiO molecules per cm$^3$. Figure 8 is a plot of $n_{eff}$ for NiO. At higher energies, $n_{eff}$ should finally saturate at a value of 14 (assuming deeper valence levels are not excited) corresponding to 8 valence electrons of the nickel ion and 6 for the oxygen ion of each NiO molecule. The fact that $n_{eff}$ rises so slowly indicates that optical transition strengths are relatively small in the spectral region of study.

## IV. CoO EXPERIMENTAL RESULTS

### A. CoO Reflectance Spectrum

The absolute reflectance of CoO was measured on two cleaved samples for photon energies from 1.0 to 26.8 eV. Absolute reflectance was also measured using the beam of helium-neon laser

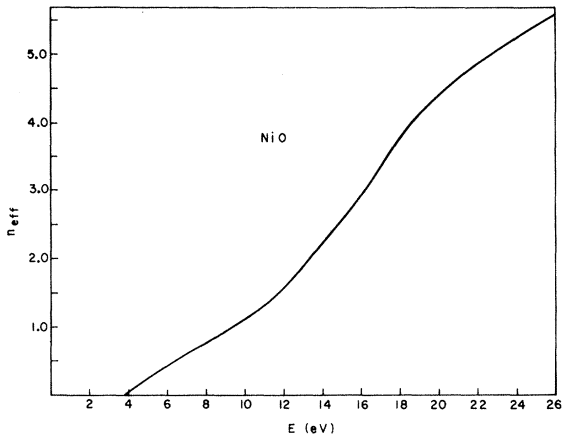


FIG. 8. Effective number of electrons per NiO unit contributing to optical absorption.

(1.96 eV) and a silicon solar-cell detector in order to provide a check on the chamber measurements and give an accurate value for the optical dielectric constant.

The spectrum of reflectance from a cleaved CoO crystal is shown in Fig. 9. The first reflectance peak occurs at $\hbar\omega = 5.5$ eV, where the reflectance reaches its maximum of 20%. (The splitting of this peak shown in Fig. 9 is subject to some doubt, since it was not resolved in the second sample.) Proceeding to higher energies, we find a shoulder at $\hbar\omega = 7.5$ eV, a peak at $\hbar\omega = 12.6$ eV, and a final peak at $\hbar\omega = 17.5$ eV.

The data points obtained in the CoO measurements were the same as in the NiO measurements. Therefore, the details are accurately known for $\hbar\omega \leq 14.4$ eV, but the detailed nature of reflectance (i.e., the possibility of additional structure in some energy ranges) for $\hbar\omega > 14.4$ eV is not certain. The extrapolation used in the Kramers-Krönig analysis was similar to that used for NiO.

### B. Optical Constants of CoO

The optical constants of CoO are presented in Figs. 10 and 11. Figure 10 gives the real ($n$) and imaginary ($k$) parts of the complex refractive index ($N = n - ik$), and Fig. 11 depicts the real ($\epsilon_{1r}$) and imaginary ($\epsilon_{2r}$) parts of the complex relative dielectric constant ($\epsilon_r = \epsilon_{1r} - i\epsilon_{2r}$). As in the NiO results, the low-energy values of $n$ and $\epsilon_{1r}$ differ somewhat for those obtained by other workers, and Table II summarizes the values for the refractive index and optical dielectric constant determined from the present work and the values previously reported. The values obtained in this work are averages of several cleaved crystals and are believed to be accurate to within ±3% (at $\hbar\omega = 2.0$ eV).

The CoO optical-absorption coefficient is presented in Fig. 12. The photon energies at which structure shows are marked by the arrows in the figure. As expected, the positions of the structure in the absorption coefficient are somewhat different from those of the reflectance spectrum of Fig. 9.

## V. DISCUSSION

It is important to the discussion of the optical properties that we establish the nature of the occupied states which contribute to optical transitions. These states must be associated with either or both of the nickel ion $3d^8$ levels or the oxygen ion $2p^6$ levels since other filled levels are sufficiently removed in energy that they need not be considered in optical excitations.[22] Evidence for the

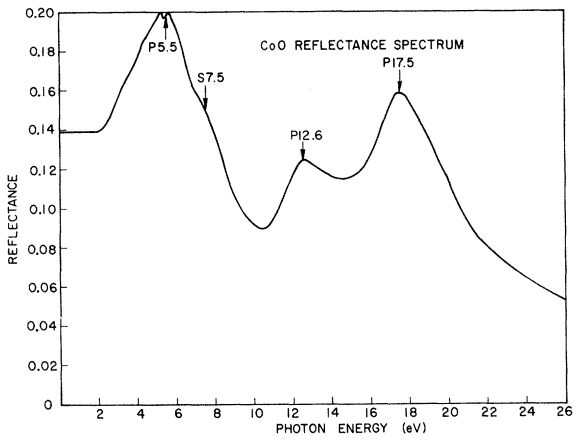


FIG. 9. Reflectance spectrum of CoO.

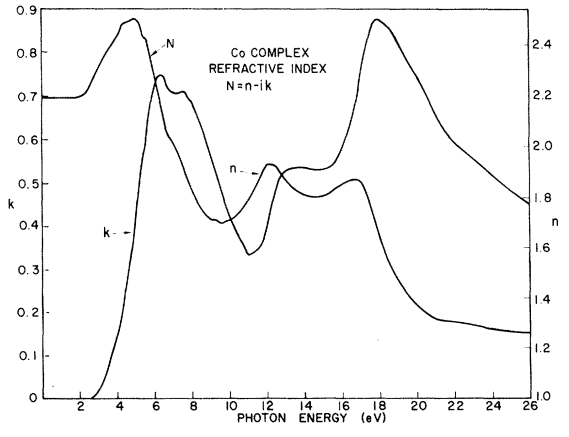


FIG. 10. Real and imaginary parts of the CoO complex refractive index.

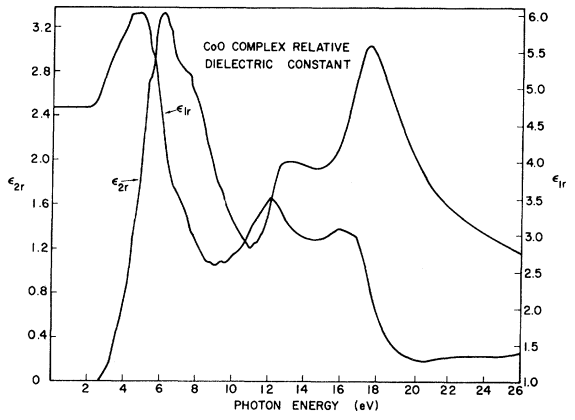


FIG. 11. Real and imaginary parts of the CoO complex relative dielectric constant.

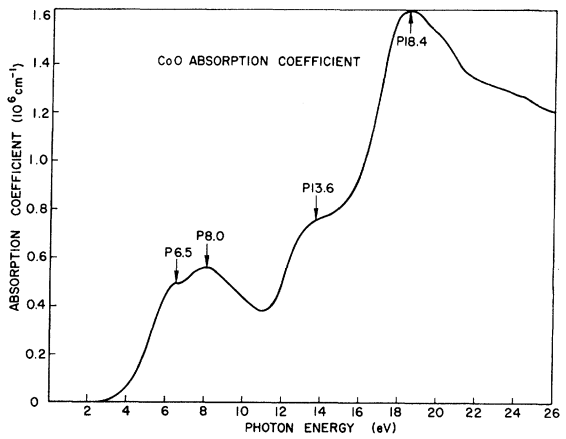


FIG. 12. Optical-absorption coefficient of CoO.

nature of the $3d^8$ levels in NiO has been provided by studies of the crystal-field spectra[23] of the $Ni^{2+}$ ion. It has been observed that the spectra of the $Ni^{2+}$ ion in an octahedral crystal field are qualitatively identical for many materials, and the quantitative differences, which stem from differences in the strength of the crystal field, are small. For example, Newman and Chrenko[13] have found the location and strength of absorption lines in the crystal-field spectrum of the $Ni^{2+}$ ion in NiO to be identical (within experimental error) with lines in the spectrum of $Ni^{2+}$ in MgO (as an impurity) measured by Low[24] and very similar to lines in the spectrum of the complex Ni $(H_2O)_6^{++}$.[25]

The fact that the spectra of $Ni^{2+}$ in NiO can be explained in terms of this point-ion model implies that the $3d$ wave functions are highly localized and that local (or site) symmetry rather than translational symmetry is the most relevant to the $3d$ electrons in this material.

Regarding the states associated with the oxygen-ion $2p^6$ levels, there is experimental evidence from x-ray emission spectra[26] and theoretical evidence from band-structure calculations[27] that the oxygen $2p$ wave functions overlap sufficiently in NiO to form an energy band several eV in width.

Having discussed evidence for the nature of the relevant occupied states, let us consider possible interpretations of the absorption edge at 3.7 eV and the structure in the absorption coefficient below 9.0 eV. First, let us assume that the transitions producing this structure originate primarily from the oxygen $2p$ band.

It has been suggested[13] that the sharp rise in the absorption of NiO near $\hbar\omega = 4.0$ eV is the onset of "charge-transfer transitions." The concept of charge transfer in solids is one which has been carried over from the study of electronic excitation in molecules.[28] The charge-transfer model was applied in early studies of the alkali halides[29] to explain the nonconducting excited states. In this model an electron is removed from the negative ion and placed on a nearest-neighbor positive ion. The aforementioned crystal-field spectrum of NiO plus the studies of the nature of the charge-transfer spectra in transition-metal complexes[30] provide some of the justification for the extension of the charge-transfer concept to solids such as NiO. In solids, a charge-transfer excitation corresponds to the formation of a "transfer exciton." In the transfer exciton, the excited electron is assumed to be associated with one of the nearest-neighbor (or next-nearest-neighbor) positive ions. The

TABLE II. Refractive index and optical dielectric constant of CoO.

| Refractive Index $n$ | Optical dielectric constant $\epsilon_{1r}=n^2$ | Method | Ref. |
|---|---|---|---|
| 2.33 | 5.35 | Infrared reflectance (1 $\mu$) (experimental) | 16 |
| 2.30 | 5.3 | Calculated from damped oscillator model applied to lattice vibrational spectrum | 17 |
| 2.51 | 5.01 | Calculated from damped oscillator model applied to lattice vibrational spectrum | 18 |
| 2.18 | 4.76 | Reflectance ($\hbar\omega = 2.0$ eV) | Present work |

transferred electron may go into $3d$ or other (say, $4s$) orbitals on the $Ni^{2+}$ ion, and since it is equally likely to be on any one of six nearest-neighbor $Ni^{2+}$ ions, its wave function must be represented by a symmetrically appropriate (i.e., it must agree with the crystal symmetry) linear combination of atomic functions centered on the nearest neighbors. Overhauser[31] has used group-theoretical techniques to evaluate the symmetrically allowable excited states for various transfer exciton configurations.

Another localized exciton model is the so-called "excitation model." Here the electron is considered to remain explicitly centered at the site of the hole, with its angular distribution described by atomic wave functions ($s$, $p$, $d$, etc.). Knox and Inchauspe[32] have pointed out that there is a fundamental correspondence between the two models and that the number of absorption lines predicted by either model is the same for a particular configuration.

The five peaks in the absorption coefficient of NiO (Fig. 6) from 4.3 to 8.5 eV may be associated with the various transitions of the $p^5d$ localized exciton.[33] Although such a $p \rightarrow d$ transition is allowed and could produce the observed absorption, the transition strength is expected to be somewhat reduced because the $d$ levels are mostly occupied, having only two empty states per $Ni^{2+}$ ion. This might explain why the effective number of electrons per NiO molecule has reached only about 1.5 for $\hbar\omega = 10$ eV (Fig. 8). The contribution of the $p$ electrons to $n_{\text{eff}}$ should reach a maximum of 6 at high energies. Doyle and Lonergan[19] have calculated the energy of a transfer excitation for both NiO and CoO using a rather crude atomic calculation; their values are 6.5 and 6.9 eV for NiO and CoO, respectively. Including the effects of crystal-field energies could reduce these values by 1–2 eV, so they are reasonably close to the first maxima in the absorption spectra (in view of the uncertainty associated with such a calculation) of NiO (4.3 eV) and CoO (6.5 eV).

When an electron is transferred to a $Ni^{2+}$ ion, thus forming a $Ni^{+}$ ion, the states of the $d$ electron are split into two groups, $d_t$ and $d_e$, corresponding to the $t$ and $e$ orbitals of $d$ electrons in an octahedral crystal field. It is interesting, though perhaps fortuitous, that the separation of the first two absorption peaks (0.6 eV) is nearly the predicted crystal-field splitting of the $3d^9$ configuration ($10Dq = 0.57$ eV).

Knox and Inchauspe have pointed out that group theory predicts seven absorption lines for the configuration $p^5d$. However, it would be pointless to attempt assignment of any of the structures in Fig. 6 to such a model, since no quantitative theoretical calculations have been made.

Feinleib and Adler[34] have proposed a model for the energy levels and bands of NiO in which they suggest that the absorption edge near 4 eV may be due to the onset of transitions from either the $2p$ band or the $3d^8$ levels to the $4s$ band. However, the latter appears to be more likely in view of the relatively small transition strength in this energy range.

McNatt[35] has proposed a model based on an energy-band calculation by Wilson[36] in which the absorption edge and higher-lying structure is the result of transitions from a mixed $p$-$d$ band to the lowest unfilled $d$ band. A major difficulty with this model is that the crystal-field spectra described above strongly indicate small $p$-$d$ interaction, and certainly the $d$-$d$ crystal-field excitations cannot be explained in terms of a one-electron band model. On the basis of the observed crystal-field spectra, we feel that a one-electron band model for the nickel $d$ states is unrealistic.

Let us now consider the possibility that the absorption and structure below 9 eV result from transitions originating from the nickel ion $3d^8$ levels. We will postpone until later consideration of the final state in such a transition. When an electron is optically excited out of a $3d^8$ state to a higher-energy level, the "hole" left behind is a $Ni^{3+}$ with electron configuration $3d^7$. The fact that this $3d^7$ configuration remaining could be in an excited state gives rise to the possibility that structure in the optical properties results from such an excitation. The excitation of lowest energy corresponds to transferring an electron from a $3d^8$ configuration (assumed in the ground state) to a higher band (non-$d$), leaving the $3d^7$ configuration in the ground state. Excited energy levels of the $3d^7$ configuration can be determined from the diagrams of Tanabe and Sugano.[37] Using the value of $B = 1115\ \text{cm}^{-1}$ given by these authors for Ni IV and a $Dq$ value of $1800\ \text{cm}^{-1}$ [22] for the $Ni^{3+}$ ion we have determined values of 0.7, 2.1, 2.8, 3.9, and 4.3 eV, respectively, for energy differences between the $^2E$, $^4F_2$, $^2F_2 + {}^2F_1$, $^4F_1$, $^4A_2 + {}^2A_1$ excited states and the $^4F_1$ ground state of the $d^7$ configuration. If we assume that the 4.2-eV peak in Fig. 6 results from a transition which leaves the $d^7$ in the ground state, then we should expect additional peaks in absorption (selection rules permitting) at $4.2 + 0.7 = 4.9$, 6.3, 7.0, 8.1, and 8.5 eV. The correspondence may be entirely coincidental, but it is apparent that five of these values are quite close to the peaks observed in Fig. 6.

Let us return now to consideration of the final state in transitions originating from the $3d^8$ levels. The first fully allowed transition of the $Ni^{2+}$ ion is $3d^8 \rightarrow 3d^7 4p$ with an energy of 13.7 eV.[38] This energy will be reduced somewhat ($\sim 2$ eV) in the

crystal because of difference in the crystal-field stabilization of the $d^8$ and $d^7$ configurations. However, reduction of this transition to about 4.3 eV seems very unlikely. On the basis of the data presented here and other experimental data, Adler and Feinleib[39] have recently indicated preference for the second alternative of their model,[34] namely, that the absorption edge arises from $3d^8 \rightarrow 4s$-band transitions. Since band-structure calculations indicate that the $4s$ band is the lowest-lying completely empty band, this interpretation appears to be the most likely if the initial states are the nickel $3d^8$ levels rather than the oxygen $2p$. Although such a $d \rightarrow s$ transition is forbidden in a free ion, the band-structure calculation of Switendick[27] indicates that the wave functions in the "$4s$" band are comprised of about 50% plane wave, 15% oxygen $p$, and ~2% nickel $p$ wave function. Thus, there is sufficient admixture of $p$ and plane wave functions in "$4s$" band to partially break down the selection rule. However, such a transition is not expected to be as strong as a fully allowed transition. It should be noted that a relatively weak transition is consistent with the small value of $n_{eff}$ (Fig. 8) below 9.0 eV since the total contribution of the $d$ electrons alone must reach 8 at high energies.

We have presented two alternative interpretations to explain the absorption edge and structure below 9 eV. The first interprets these features as a localized excitation involving oxygen $2p$ and nickel $3d$ states. In the second model excitations are from $3d^8$ initial states into the "$4s$" band, leaving the $3d^7$ "hole" in various states of excitation to give rise to the observed structure. In the first model the excitations are localized and no photoconductivity near 4 eV is expected (at higher photon energies photoconductivity might occur due to autoionization), whereas the second predicts photoconduction due to excitation of electrons into the $4s$ band. Hence, the presence or absence of photoconductivity near the absorption edge could, in principle, distinguish between the two models. An attempt to observe photoconductivity in flame-fusion-grown NiO crystals gave negative results.[22] Ksendzov and Drabkin reported the observation of photoconduction near 4 eV in a halide-decomposition NiO crystal.[40] However, we have reason to believe that the photoresponse reported may not be simple photoconductivity. Experiments have been performed on a halide-decomposition NiO single-cystal sample (resistivity ~$10^{12}$ Ω cm at 300 °K). Using a 0.25-mm-thick NiO sample with Au electrodes on opposite faces and illuminating through one Au (semitransparent) electrode, no photocurrents either transient (equipment response time $< \frac{1}{25}$ sec) or steady state were detectable ($<10^{-13}$ A) with an applied field of 4 kV/cm (either polarity) and an incident-light flux ($\hbar\omega = 5$ eV) of $5.6 \times 10^{13}$ photons/sec. With a lateral structure consisting of two Au electrodes on the same surface of the crystal a 300 °K photoresponse similar to that reported by Ksendzov and Drabkin was obtained when the surface between the electrodes was illuminated. The 300 °K dark current and the maximum photoresponse current ($\hbar\omega = 5$ eV) were both approximately $4 \times 10^{-10}$ A and both currents were polarity independent and linear with electrode potential difference. However, both the photoresponse and dark current vanished ($< 10^{-13}$ A) at 78 °K. While not clearly understood, these results seem inconsistent with the presence of ordinary (band-to-band) photoconductivity suggested by the model of Feinleib and Adler. Trapping effects may be involved in the quenching of photoconductivity at low temperature. However, it has not been established that the observed photoresponse is not merely due to thermal generation of free carriers near the surface by local heating.

Photoconductivity in the infrared has been reported recently by Tsu *et al.*[41] A sharp peak in photocurrent was observed at 0.23 eV in disordered NiO films. However, this result is not understood since it was not observed in single-crystal NiO.

These authors also observed a photoresponse extending to 4 eV, but Tsu[42] has indicated that his photoresponse does not have the appearance of simple photoconductivity, being a small effect with a long response time. It is apparent that until some of the ambiguities concerning the nature of the photoresponse have been resolved, the presence of "photoconductivity" remains a rather weak piece of evidence for distinguishing between models for the electronic structure of NiO.

Photoemission studies of NiO[22] provide evidence that the structure at 13–13.8 and 17.6 eV in Fig. 6 is due to transitions from peaks in the optical density of states at −5.8 and −9.2 eV, respectively (energies referred to the uppermost occupied state) to a peak in the optical density of states at +7.5 eV. Feinleib and Adler[34] have interpreted the 17.6-eV peak in our optical data to be a transition in which an electron is transferred from one $Ni^{2+}(3d^8)$ ion to another leaving a $Ni^{+}(3d^9)$ and a $Ni^{+}(3d^7)$. Their model places the $3d^8$ level at −1.5 eV and the $3d^9$ level at 15 eV. This interpretation is not supported by the photoemission data. Furthermore, it is very unlikely in view of the strong absorption peak since such a transition is forbidden in first order.

A comparison of Figs. 6 and 12 shows the low-energy structure in the CoO optical data to be similar to that of NiO, and the structure might be similarly interpreted, but since relatively little experimental or theoretical work on CoO has been done

to date, no further interpretation will be attempted at the present time. However, with regard to the high-energy structure, photemission data predict structure of 13.6, 15, 16.6, and 18 eV. The peaks in Fig. 12 at 13.6 and 18.4 eV are consistent with this, and the absence of resolvable structure at 15 and 16.6 eV may be due to optical selection rules or the coarseness of the reflectance data in this region. As a final observation regarding CoO, it is noted that the optical properties of CoO are (as expected) very similar to the corresponding properties of NiO. However, all observable structure is much sharper in NiO than in CoO. It is interesting that this difference agrees qualitatively with the fact that the $d$ orbitals are more tightly bound in NiO than in CoO because the larger nuclear charge on the $Ni^{2+}$ ion more than offsets the repulsive effect of the additional $d$ electron, resulting in less $d$-orbital overlap in NiO.[25] Consequently, one would expect less energy-level broadening in NiO and also that the energy levels would maintain more of their atomic nature.

## ACKNOWLEDGMENTS

One of the authors (R. J. P.) wishes to acknowledge the financial support of Sylvania Electric Products, Inc., of Mountain View, Calif., during the course of this work. Thanks are also expressed to Dr. J. L. Shay for writing the Kramers-Krönig computer program, to Dr. C. S. Sahagian of the U. S. Air Force Cambridge Research Laboratories for supplying our first flame-fusion NiO crystal, and to Dr. T. L. Weininger of General Electric Research Laboratory for supplying the halide-decomposition NiO crystal.

## APPENDIX: KRAMERS-KRÖNIG ANALYSIS

The technique of Kramers-Krönig analysis is based upon dispersion relations which are simple integral formulas relating dispersion and absorption. These formulas, which are often named after Kramers and Krönig because of their x-ray dispersion work,[43] have been applied extensively in the past to optical properties[1-7] and linear network theory.[44] These relationships are based on the fact that the real and imaginary parts of a bounded causal linear system function are not independent, but related through an integral equation. The relationship between phase $\theta(\omega)$ and attenuation $A(\omega)$ is given by[43]

$$\theta(\omega_0) = (2\omega_0/\pi) \int_0^\infty [A(\omega)/(\omega^2 - \omega_0^2)]d\omega. \quad \text{(A1)}$$

It follows from Eq. (A1) that if $A(\omega)$ is known over the entire frequency spectrum, $\theta$ may be determined at a given frequency $\omega_0$. The function to which Eq. (A1) will be applied for our purpose is the Fresnel reflection coefficient for normal incidence $r(\omega)$ which is related to the complex refractive index $N = n - ik$ by

$$r = (N-1)/(N+1) = |r| e^{i\theta}. \quad \text{(A2)}$$

The Fresnel reflection coefficient is the ratio of incident and reflected amplitudes, but the experimental quantity is the reflectance $R$, which is given by

$$R = |r|^2 = [(n-1)^2 + k^2]/[(n+1)^2 + k^2]. \quad \text{(A3)}$$

Substituting the real and imaginary parts of the complex function $\ln r = \ln|r| + i\theta$ into Eq. (A1) and using (A3), we have

$$\theta(\omega_0) = (\omega_0/\pi) \int_0^\infty [\ln R(\omega)/(\omega^2 - \omega_0^2)]d\omega. \quad \text{(A4)}$$

The success of the Kramers-Krönig analysis method depends on the fact that negligible error results from a lack of knowledge of the reflectance far removed from the frequency of interest. This becomes more apparent if Eq. (A4) is written in an alternative form derivable from (A4) by integrating by parts:

$$\theta(\omega_0) = \frac{1}{2\pi} \int_0^\infty \frac{d\ln R}{d\omega} \ln\left|\frac{\omega+\omega_0}{\omega-\omega_0}\right| d\omega. \quad \text{(A5)}$$

The logarithmic weighting function in (A5) becomes small for frequencies far removed from $\omega_0$ and thus reduces the relative contribution to the integral at such frequencies. Furthermore, $\ln R$ appears in a derivative in the integrand, so there is no contribution from a region of constant reflectance, and positive and negative slopes on the same side of $\omega_0$ (e.g., the slopes of a peak at a remote point) tend to cancel each other.

Bode's method for the determination of the phase associated with a known attenuation characteristic has been applied extensively in the field of linear circuit analysis.[15,44] The first application of this method to optical spectra was apparently made by Kreiger, Olechna, and Story,[45] who wrote FORTRAN programs applying the technique to reflectance spectra. The method of Bode is basically a conceptually rewarding and mathematically convenient way of performing the integration of Eq. (A5). The conceptual significance of this method is best appreciated through a study of the paper of Thomas.[15] Briefly stated, the method involves connecting experimental points by straight lines on a $\ln|R|$-versus-$\ln\omega$ plot. Then the phase for a given value of $\omega$ (say, $\omega_0$) is determined by summing the phase contributions of individual line segments. The phase in radians at $\omega_0$ corresponding to a semi-infinite unit slope of attenuation starting at $\omega$ is given by Bode as

$$\Phi(x)=B(x), \quad x=\omega_0/\omega, \quad x<1$$
$$\Phi(x)=\tfrac{1}{2}\pi - B(x), \quad x=\omega/\omega_0, \quad x<1 \tag{A6}$$
$$B(x)=\frac{2}{\pi}\sum_{m=1}^{\infty}\frac{x^{(2m-1)}}{(2m-1)^2}, \quad \Phi(1)=\tfrac{1}{4}\pi \ .$$

The derivative of Eq. (A6) is expressible in closed form[15]

$$\frac{d\Phi}{dx} = \pm\frac{1}{\pi x}\ln\left|\frac{1+x}{1-x}\right|, \tag{A7}$$

where the positive sign is taken for $x=\omega_0/\omega$ and the negative sign for $x=\omega/\omega_0$. Substituting (A7) into (A5), we get for either choice of $x$

$$\theta(\omega_0) = -\frac{1}{2}\int_0^{\infty}\frac{d\ln R}{d\ln\omega}\,d\Phi \ . \tag{A8}$$

Expressing Eq. (A8) as a finite sum, [46] we get

$$\theta(\omega_0)=\frac{1}{2}\sum_{i=1}^{M}k_i[\Phi(x_i)-\Phi(x_{i+1})],$$
$$k_i=\frac{\ln|R_{i+1}|-\ln|R_i|}{\ln\omega_{i+1}-\ln\omega_i}, \tag{A9}$$

where $x_i=\omega_0/\omega_i$ for $\omega_i>\omega_0$ and $x_i=\omega_i/\omega_0$ for $\omega_i<\omega_0$ as in Eq. (A6).

Equations (A9) in conjunction with (A6) are in a form suitable for computer programming. The $R_i$ and $\omega_i$ are the discrete experimental reflectance values and frequencies (photon energies), respectively. One additional modification is useful to help reduce computation time. The series in Eq. (A6) is rather slowly convergent for $x$ near unity. Kreiger *et al.* found it useful to use the following:

$$B(x)=\tfrac{1}{4}\pi-\frac{1}{\pi}\ln x\left(\frac{1-x}{1+x}\right)-\frac{2}{\pi}\sum_{1}^{\infty}\left[\left(\frac{1-x}{1+x}\right)^{(2m-1)}\right.$$
$$B(x)=\frac{2}{\pi}\sum_{1}^{\infty}\frac{x^{(2m-1)}}{(2m-1)^2} \quad \text{for } 0\le x\le(\sqrt{2}-1),$$
$$\left.(2m-1)^2\right] \quad \text{for } (\sqrt{2}-1)<x<1. \tag{A10}$$

The latter form may be derived by substitution of $y=(1+x)/(1-x)$ into Eq. (A7) and integrating by parts. The value $(\sqrt{2}-1)$ arises because it is the value of $x$ for which both series have the same argument.

Having determined a value of $\theta$ for a given photon energy the real and imaginary parts of the complex refractive index $(n-ik)$ are obtained from[47]

$$n=(1-|r|^2)/(1+|r|^2-2|r|\cos\theta)\,, \tag{A11}$$

$$k=(n+1)\,|r|\sin\theta/(|r|\cos\theta-1)\,. \tag{A12}$$

The real and imaginary parts of the complex relative dielectric constant $(\epsilon_{1r}-i\epsilon_{2r})$ and the absorption coefficient $\alpha$ are determined by

$$\epsilon_{1r}=n^2-k^2, \quad \epsilon_{2r}=2nk, \quad \alpha=4\pi k/\lambda\,. \tag{A13}$$

---

†Work supported by the U.S. Army Research Office (Durham) and by the Advanced Research Projects Agency through the Center for Materials Research at Stanford University.

*Paper based in part on a thesis submitted by R. J. Powell to Stanford University in partial fulfillment of the requirements of the Ph.D. degree.

‡Present address: Bell Telephone Laboratories, Murray Hill, N. J. 07974.

[1]H. R. Philipp and E. A. Taft, Phys. Rev. 113, 1002 (1959).

[2]J. Tauc and A. Abraham, in *Proceedings of the International Conference on Semiconductor Physics, Prague*, 1960 (Academic, New York, 1961).

[3]H. Ehrenreich, H. R. Philipp, and J. C. Phillips, Phys. Rev. Letters 8, 59 (1962).

[4]M. Cardona and D. L. Greenaway, Phys. Rev. 125, 1291 (1962).

[5]M. Cardona and D. L. Greenaway, Phys. Rev. 131, 98 (1963).

[6]H. R. Philipp and H. Ehrenreich, Phys. Rev. 129, 1550 (1963).

[7]M. Cardona and D. L. Greenaway, Phys. Rev. 133, A1685 (1964).

[8]C. N. Berglund and W. E. Spicer, Phys. Rev. 136, A1030 (1964); 136, A1044 (1964).

[9]N. B. Kindig and W. E. Spicer, Phys. Rev. 138, A561 (1965).

[10]A. J. Blodgett, Jr., and W. E. Spicer, Phys. Rev. Letters 15, 29 (1965).

[11]J. L. Shay and W. E. Spicer, Phys. Rev. 161, 799 (1965).

[12]R. C. Eden, Ph.D. thesis, Stanford University, 1967 (unpublished).

[13]R. Newman and R. M. Chrenko, Phys. Rev. 114, 1507 (1959).

[14]Because of the nature of the logarithmic weighting factor in the Kramers-Krönig integral (see Appendix), structure in the optical constants is little affected by values of or changes in reflectance which are sufficiently far removed in frequency. Consequently, although the reflectance actually has some strong structure due to lattice vibrational absorption in the infrared (near 0.1 eV), this has a negligible effect on the optical constants determined above $\hbar\omega=1.0$ eV.

[15]D. E. Thomas, Bell System. Tech. J. 26, 870 (1947).

[16]K. V. Rao and A. Smakula, J. Appl. Phys. 36, 2031 (1965).

[17]P. J. Gielisse *et al.*, J. Appl. Phys. 36, 2446 (1965).

[18]R. Marshall *et al.*, in *Proceedings of the Seventh*

*International Conference on the Physics of Semiconductors, Paris*, 1964 (Academic, New York, 1965).

[19]W. P. Doyle and G. A. Lonergan, Discussions Faraday Soc. 26, 27 (1958).

[20]C. E. Rossi and W. Paul, J. Phys. Chem. Solids 30, 2295 (1969).

[21]H. R. Philipp and H. Ehrenreich, Phys. Rev. 129, 1550 (1963).

[22]R. J. Powell, Ph.D. thesis, Stanford University, 1967 (unpublished); R. J. Powell and W. E. Spicer (unpublished).

[23]The term "crystal-field spectra" refers to the spectra of optical transitions within the *d* levels of a transition-metal ion, which are split by the electric field of the nearest-neighbor anions. It is found that these spectra are explained when the anions are treated as point charges.

[24]W. Low, Phys. Rev. 109, 247 (1958).

[25]F. J. Morin, in *Semiconductors*, edited by N. B. Hannay (Reinhold, New York, 1959).

[26]D. Coster and S. Kiestra, Physica 14, 175 (1948).

[27]A. C. Switendick, Ph.D. thesis, M.I.T., 1963 (unpublished).

[28]C. K. Jorgensen, *Absorption Spectra and Chemical Bonding in Complexes* (Pergamon, Oxford, 1962).

[29]N. F. Mott and R. W. Gurney, *Electronic Processes in Ionic Crystals* (Oxford U. P., London, 1948), 2nd ed.

[30]D. S. McClure, *Electronic Spectra of Molecules and Ions in Crystals* (Academic, New York, 1959).

[31]A. W. Overhauser, Phys. Rev. 101, 1702 (1956).

[32]R. S. Knox and N. Inchauspe, Phys. Rev. 116, 1093 (1959).

[33]In this excitation an electron is removed from an oxygen ion $p^6$ shell, leaving a $p^5$ hole, and excited to a *d* orbital on a $Ni^{2+}$ ion (transfer model) or a *d* orbital centered on the site of the $p^5$ hole (excitation model), hence the description $p^5d$. Note that in the transfer model the nickel ion changes from a $3d^8$ to a $3d^9$ configuration.

[34]J. Feinleib and D. Adler, Phys. Rev. Letters 21, 1010 (1968).

[35]J. L. McNatt, Phys. Rev. Letters 23, 915 (1969).

[36]T. M. Wilson, Oklahoma State University, Quantum Theoretical Research Group, Research Note No. 1, 1969 (unpublished).

[37]Y. Tanabe and S. Sugano, J. Phys. Soc. Japan 9, 766 (1954).

[38]C. E. Moore, *Atomic Energy Levels*, Natl. Bur. Stds. (U.S.) Circ. 467, (GPO, Washington, D. C., 1949, 1952, and 1958), Vols. I, II, and III.

[39]Proceedings of the Electronic Density of States Conference, National Bureau of Standards, Gaithersburg, Md., 1969 (unpublished).

[40]Ya. M. Ksendzov and I. A. Drabkin, Fiz. Tverd. Tela 7, 1519 (1965) [Soviet Phys. Solid State 7, 1220 (1965)].

[41]R. Tsu, L. Esaki, and R. Ludeke, Phys. Rev. Letters 23, 977 (1969).

[42]R. Tsu (private communication).

[43]See F. Stern, in *Solid State Physics* (Academic, New York, 1963), Vol. 15, p. 299.

[44]H. W. Bode, *Network Analysis and Feedback Amplifier Design* (Van Nostrand, Princeton, N. J., 1945).

[45]E. L. Kreiger, D. J. Olechna, and D. S. Story, General Electric Research Lab. Report No. 63-RL-3458G, 1963 (unpublished).

[46]In making the sum finite we are, of course, making an assumption common to all Kramers-Krönig analyses, viz., that the known values of *R* extend to regions of constant *R* or can be suitably extrapolated to such a region.

[47]T. S. Moss, *Optical Properties of Semiconductors* (Butterworth, London, 1961).